



HAL
open science

LPCVD of Al₂O₃ layers using a hot-wall reactor

C. Labatut, C. Combescure, B. Armas

► **To cite this version:**

C. Labatut, C. Combescure, B. Armas. LPCVD of Al₂O₃ layers using a hot-wall reactor. Journal de Physique IV Proceedings, 1993, 03 (C3), pp.C3-589-C3-596. 10.1051/jp4:1993381 . jpa-00251438

HAL Id: jpa-00251438

<https://hal.science/jpa-00251438>

Submitted on 4 Feb 2008

HAL is a multi-disciplinary open access archive for the deposit and dissemination of scientific research documents, whether they are published or not. The documents may come from teaching and research institutions in France or abroad, or from public or private research centers.

L'archive ouverte pluridisciplinaire **HAL**, est destinée au dépôt et à la diffusion de documents scientifiques de niveau recherche, publiés ou non, émanant des établissements d'enseignement et de recherche français ou étrangers, des laboratoires publics ou privés.

LPCVD of Al₂O₃ layers using a hot-wall reactor

C. LABATUT, C. COMBESURE and B. ARMAS

Institut de Science et de Génie des Matériaux et Procédés, CNRS-IMP, BP. 5, Odeillo, 66125 Font Romeu cedex, France

ABSTRACT:

We have studied the chemical vapour deposition of alumina (Al₂O₃) using aluminium chloride (AlCl₃) as a source of aluminium and nitrous oxide (N₂O) or carbon dioxide (CO₂) as the oxygen vector. We also used hydrogen (H₂) and a carrier gas (N₂). A preliminary thermodynamic study indicated the influence of temperature, total pressure of the reactants and the composition of the gas mixture. The synthesis of the alumina deposited was carried out in a hot-wall reactor at temperatures between 1000 and 1300°C and at pressures varying from 133 to 665 Pa. All deposits were crystallised and adherent to the substrates of silicon carbide (SiC) or aluminium nitride (AlN). The structure and crystallographic orientation of the Al₂O₃ films were investigated by X-ray diffraction. Particular attention was paid to the morphology of the deposits. Observations were made with the help of a Scanning Electron Microscope (SEM). Two studies were carried out as a function of temperature, one for the deposits made from nitrous oxide and the other for those made using carbon dioxide. The crystal size of Al₂O₃ increases with temperature but, more importantly, the crystal habit changes too.

1. INTRODUCTION

For many years, chemically vapour-deposited Al₂O₃ film has been chosen as the coating material for improving the wear resistance of cutting tools and for lightweight transparent armour applications. For these applications, Al₂O₃ layers were deposited in a cold or hot wall reactor from AlCl₃-H₂-CO₂ [1,7].

For semiconductor device applications, an organometallic precursor (Al(C₃H₇O)₃) has been chosen to elaborate Al₂O₃ [8-10].

Nitrous oxide as an oxygen source was used only with aluminum trimethyl to elaborate Al₂O₃ by CVD [11].

Here, alumina has been studied as an oxidation-resistant product. Thus, we were looking for a high-compacity deposit with good adherence of the layers to the substrate. For this, we had to examine the morphology.

In order to work under industrial conditions, we chose to elaborate our deposits in a hot wall reactor.

It is possible to vary four parameters: total pressure, the

precursors, the supersaturation and the temperature.

The total pressure was maintained at a low value (1 to 5 Torr) in order to eliminate the risk of a nucleation in the homogeneous phase.

Two oxygen sources, nitrous oxide and carbon dioxide, were used.

The supersaturation and the temperature are the principal factors controlling the nucleation and the resultant structures of the deposits. In a hot wall reactor, one cannot work with an high supersaturation of the reactants. Thus, we studied the influence of the deposition temperature in two systems $\text{AlCl}_3\text{-N}_2\text{O-H}_2$ and $\text{AlCl}_3\text{-CO}_2\text{-H}_2$. This parameter is an especially critical factor related to adsorbed atomic or molecular mobility, which influences the growth morphology.

The present work firstly examines the theoretical possibility of having an alumina coating with the help of the thermodynamic study of the two preceding systems. For $\text{AlCl}_3\text{-CO}_2\text{-H}_2$ and for a high total pressure, this system has already been the object of several studies [12,13].

Secondly, we experimentally observed the evolution of the growth morphology with temperature.

2. THERMODYNAMIC STUDY

Two systems were investigated Al-Cl-N-O-H-Ar and Al-Cl-C-O-H-Ar .

The composition of the equilibrium phases was first determined by a thermodynamic calculation. Thermodynamic calculations based on the minimization of the total Gibbs free energy of a system were carried out using the computer program "SOLGASMIX" developed by ERIKSSON [14].

In the following analysis, it was assumed that the substrate is chemically inert towards both the alumina deposit and the vapour phase. For this calculation, it was assumed that the system was in equilibrium and that all the chemical species able to be present at equilibrium were known and taken into account.

For $\text{AlCl}_3\text{-N}_2\text{O-H}_2$, 56 species were considered (table 1) and for $\text{AlCl}_3\text{-CO}_2\text{-H}_2$, 55 (table 2).

For the two systems, the thermodynamic data used for the calculation was taken from JANAF, BARIN tables and for the aluminium oxynitride ($\text{Al}_7\text{O}_9\text{N}$) the values are KAUFMAN's[15].

The domain of investigation is: $0.01 \leq \text{N}_2\text{O}/\text{AlCl}_3 \leq 100$ or $0.01 \leq \text{CO}_2/\text{AlCl}_3 \leq 100$, $0.01 \leq \text{H}_2/\text{AlCl}_3 \leq 100$, $1200 \leq T \leq 1800$ K and $10^{-3} \leq P \leq 5.10^{-3}$ atm (133 to 665 Pa).

Since the chemical species initially introduced into the calculations either reacted totally at equilibrium to give new species or remained partially unreacted, the results will be formulated as thermodynamic yields η_x . For example:

$$\eta_{\text{Al}_2\text{O}_3} = 200 \frac{\langle \text{Al}_2\text{O}_3 \rangle_{\text{eq}}}{\text{AlCl}_3 \text{ in}} \quad \eta_{\text{AlCl}_3} = 100 \frac{\text{AlCl}_3 \text{ eq}}{\text{AlCl}_3 \text{ in}}$$

$$\eta_{\text{HCl}} = 100 \frac{\text{HCl eq}}{3 \text{ AlCl}_3 \text{ in}} \quad \eta_{\text{CO}_2} = 100 \frac{\text{CO}_2 \text{ eq}}{\text{CO}_2 \text{ in}}$$

in which $X_{i \text{ in}}$ is the input number of moles of species X
and X_{eq} is the number of moles of species X at equilibrium.

2.1 Influence of the initial composition:

We look at the variation of η_x as a function of the initial composition ratios: $\alpha = \text{N}_2\text{O}/\text{AlCl}_3$ or $\beta = \text{CO}_2/\text{AlCl}_3$, $\kappa = \text{H}_2/\text{AlCl}_3$.

2.1.1 Yield variation as a function of the ratio of oxygen vector to aluminium chloride

- For nitrous oxide

The influence of nitrous oxide on the equilibrium composition was investigated (figure 1). Until the point where $\alpha = \alpha^* = 1.6$, as α increases, the quantity of solid Al_2O_3 increases and consequently that of the chloride decreases. After α^* , the quantity of solid Al_2O_3 stays constant and the formation is maximised. Thus, in order to obtain a good reaction yield, it is necessary to work with an excess of nitrous oxide over aluminium chloride.

- For carbon dioxide

The influence of carbon dioxide on the equilibrium composition was investigated (figure 2). We can discuss the results as a function of β which is similar to α . For the same temperature and a low pressure, the results for solid Al_2O_3 are identical to the previous study. The formation of dangerous carbon monoxide (CO) is noted whatever for all values of β and the presence of carbon dioxide when β has a high value ($\beta \geq 10$).

2.1.2 Yield variation as a function of the ratio of hydrogen to aluminium chloride

In figures 1 and 2, we have an excess of H_2 . Now, the influence of hydrogen has been studied for a value of α or β which gives a maximum yield of solid Al_2O_3 .

Figure 3 shows that κ does not change the result of the solid Al_2O_3 yield. κ only has an influence on the gaseous phase. The κ increase results progressively in the formation of H_2O and HCl , instead of O_2 and Cl_2 , in the latter phase.

In figure 4, when κ increases, the solid Al_2O_3 yield increases. With this system, we note a greater influence of hydrogen in the formation of solid Al_2O_3 .

2.2 Influence of the temperature

For $\text{Al}_2\text{O}_3\text{-N}_2\text{O-H}_2$, the temperature does not influence the solid and gaseous phases.

For $\text{AlCl}_3\text{-CO}_2\text{-H}_2$, the solid phase presents the same phenomenon. For the gaseous phase, the presence of a slight variation is noted. When the temperature increases part of the CO is transformed into CO_2 and part of the H_2 into H_2O .

3. EXPERIMENTAL STUDY

The experimental device used was a vertical hot wall reactor composed of a graphite susceptor heated by high frequency induction. Source gases were hydrogen, nitrous oxide or carbon dioxide and nitrogen. The aluminium chloride (AlCl_3) was put in an evaporator. The AlCl_3 was heated by a wire heater and carried by nitrogen. The aluminium chloride was inputted separately from the other reactive gases to avoid a reaction between them before the reaction zone. The deposits were made on graphite substrates protected by a β SiC layer deposited by CVD.

3.1 Alumina by $\text{AlCl}_3\text{-N}_2\text{O-H}_2$

The conditions were $P = 133$ Pa, the ratios $\text{N}_2\text{O}/\text{AlCl}_3 = 20$, $\text{H}_2/\text{AlCl}_3 = 150$ and $\text{N}_2/\text{AlCl}_3 = 260$ with a variation of the temperature between 1000 and 1200°C.

The X-ray diffraction patterns show that crystallised Al_2O_3 is

synthesized. As a function of the temperature, different phases are obtained. At 1000°C, a mixture of θ -Al₂O₃ and α -Al₂O₃ is obtained. α -Al₂O₃ (corundum) is the stable phase of alumina and θ -Al₂O₃ is a metastable phase. At higher temperatures, only α -Al₂O₃ is detected.

The surface morphology of the deposits has been examined by Scanning Electron Microscopy (SEM). At 1000°C, the observations of the surface show two types of crystals. Large ones ($\approx 6 \mu\text{m}$) with pyramidal and prismatic forms and small ones of 0.5 μm size (figure 7). When the temperature increases up to 1150°C, only prismatic (100 or 010) and pynacoidal (001) faces are present, the pyramidal faces have disappeared (figure 8). At 1200°C, we observed well defined crystals ($\approx 20 \mu\text{m}$) with a combination of forms formed by (110), (001) and probably (113) (figure 9). Thus, two phenomena are revealed as a function of the temperature: variation of the crystal shape and variation of the crystal size.

3.2 Alumina by AlCl₃-CO₂-H₂

The conditions are P=665 Pa, the ratios CO₂/AlCl₃=50, H₂/AlCl₃=150 and N₂/AlCl₃=260 with a variation of the temperature between 1100 and 1300°C.

The total pressure and the initial temperature are increased (665 Pa; 1100°C) to have a sufficiently high deposition rate.

The X-ray diffraction patterns show that crystallised α -Al₂O₃ is synthesized.

The surface morphology of the deposits was examined by Scanning Electron Microscopy (SEM). At 1100°C, the crystal shape is new, we do not observe this with AlCl₃-N₂O-H₂. It is a combination of pynacoidal (001) and inclined (012) faces. This deposit seems very compact, the crystal size being around 3 μm (figure 10).

At 1200°C, the crystal habit is formed of prismatic (110), pynacoidal (001) and inclined (116) or (113) faces. The surface appearance is similar to the one elaborated at 1150°C from the AlCl₃-N₂O-H₂ system (figure 11).

When the temperature increases up to 1300°C, the surface presents a disorder similar to that of the layer made at 1200°C with the nitrous oxide precursor.

The crystal shape is a result of a combination of pynacoidal (001), prismatic (110) and inclined (012), (113), (116) faces (figure 12).

4. CONCLUSION

The thermodynamic study indicates the existence fields of Al₂O₃, and shows that it is easy to obtain alumina from AlCl₃-N₂O-N₂ or from AlCl₃-CO₂-H₂ if one works with an excess of nitrous oxide or carbon dioxide over aluminium chloride.

This result is in agreement with the previous study on the AlCl₃-CO₂-H₂ system. We made a similiary study only as a comparison with the AlCl₃-N₂O-H₂ system.

In the experimental study, by varying the temperature, we have deposited alumina. From AlCl₃-N₂O-H₂ and at low temperature (1000°C), θ -Al₂O₃ has appeared. This compound is not revealed by the thermodynamic study because it is a metastable phase. In the two systems, the crystallization has a similar evolution with temperature. The deposits seem more regular at an intermediate temperature (1150 - 1200°C).

ACKNOWLEDGEMENTS

This work has been supported by AEROSPATIALE - Division Systèmes Stratégiques et Spatiaux - F33165 SAINT-MEDARD-EN-JALLES.

REFERENCES

- [1] SCHAFFER P.S., J. Am. Ceram. Soc., 48, 10, (1965), 508.
 [2] KIM J-G, PARK C-S, CHUN J.S., Thin Solid Films, 97 (1982) 97.
 [3] LUX B., COLOMBIER C., ALTENA H., Thin Solid Films, 138 (1986) 49.
 [4] WONG P., MESSIER D.R., Proc.2th Int.Conf.on CVD, (1970) 803.
 [5] KORNMAN M., SCHACHNER H., FUNK R., LUX B., J. Crystal Growth, 28 (1975) 259.
 [6] LINDSTROM J.N., JOHANNESSON R.T, J. Electrochem. Soc., 123 (1976) 555.
 [7] CHOI S.W., KIM C., KIM J.G., CHUN J.S., J. Materials Sci., 22 (1987) 1051.
 [8] SARAIE J., KWON J., YODOGAWA Y., J. Electrochem. Soc., 132 (1985) 890.
 [9] SARAIE J., ONO K., TAKEUCHI S., J. Electrochem. Soc., 136 (1989) 3139.
 [10] YOM S.S., KANG W.N., YOON Y.S., LEE J.I., Thin Solid Films, 213 (1992) 72.
 [11] HALL L., ROBINETTE B., Proc.2th Int.Conf.on CVD, (1970) 637.
 [12] COLMET R., NASLAIN R., HAGENMULLER P., BERNARD C., J. Electrochem. Soc., 129 (1982), 1367.
 [13] COLOMBIER C., LUX B., J. Materials Sci., 24 (1989) 462.
 [14] ERIKSSON G., Chemica Scripta, 8 (1975) 100.
 [15] ASPAR B., ARMAS B., COMBESURE C., THENEGAL D., J. Eur. Ceram. Soc., 8 (1991) 251.

Table 1. Chemical species introduced in the thermodynamic calculations (<> solid, //liquid, gas)

SYSTEM Al-Cl-N-H-O					
Al	AlOOH	ClO ₂	NH ₃	N ₂ O ₅	HO ₂
AlCl ₃	AlO	Cl ₂ O	N ₂ H ₂	NOH	O
AlCl ₂	AlO ₂	ClHO	N ₂ H ₄	NO ₂ H	O ₂ *
AlCl	Al ₂ O	ClNO	NO	NO ₃ H	/Al/*
Al ₂ Cl ₆	Al ₂ O ₂	ClNO ₂	NO ₂	H	<AlN>
AlOCl	Cl	N	NO ₃	H ₂ *	<Al ₂ O ₃ >
AlH	Cl ₂ *	N ₂ *	N ₂ O	H ₂ O	<Al ₇ O ₉ N>
AlN	ClH	NH	N ₂ O ₃	H ₂ O ₂	<AlCl ₃ >
AlOH	ClO	NH ₂	N ₂ O ₄	HO	<AlOCl>

Table 2. Chemical species introduced in the thermodynamic calculations (<> solid, //liquid, gas)

SYSTEM Al-Cl-C-H-O					
Al	AlO	ClHO	CH ₃ Cl	O	/Al/*
AlCl ₃	AlO ₂	COCl	CH ₄	O ₂ *	<C>*
AlCl ₂	Al ₂ O	COCl ₂	C ₂ H ₄ O	C ₂ H ₄	<Al ₂ O ₃ >
AlCl	Al ₂ O ₂	CO	C ₂ H ₂	CHO	<Al ₄ C ₃ >
Al ₂ Cl ₆	Cl	CO ₂	H	CCl	<AlOCl>
AlOCl	Cl ₂ *	C ₃ O ₂	H ₂ *	CHCl	
AlH	ClH	CCl ₄	H ₂ O	CCl ₂	
AlOH	ClO	CHCl ₃	H ₂ O ₂	CCl ₃	
AlOOH	ClO ₂	CH ₂ Cl ₂	HO	C ₂ Cl ₄	
AlC	Cl ₂ O	CH ₂ O	HO ₂	C ₂ Cl ₆	

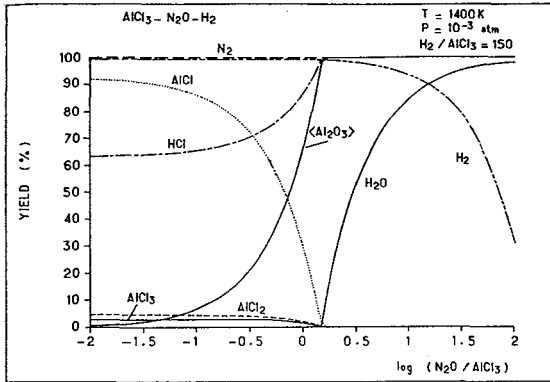


Figure 1 :
Variation of η_x equilibrium yields for the main species as a function of α with $\kappa=150$, $P=10^{-3}$ atm (101 Pa) and $T=1400K$.

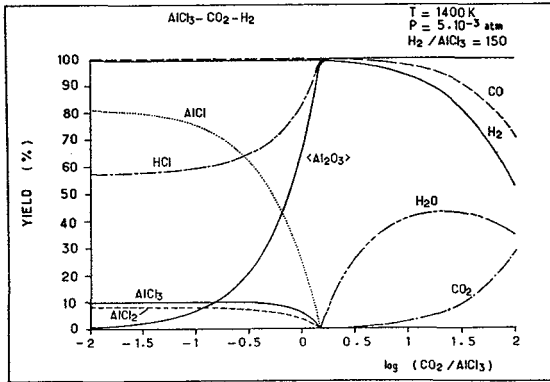


Figure 2 :
Variation of η_x equilibrium yields for the main species as a function of β with $\kappa=150$, $P=5.10^{-3}$ atm (506 Pa) and $T=1400K$.

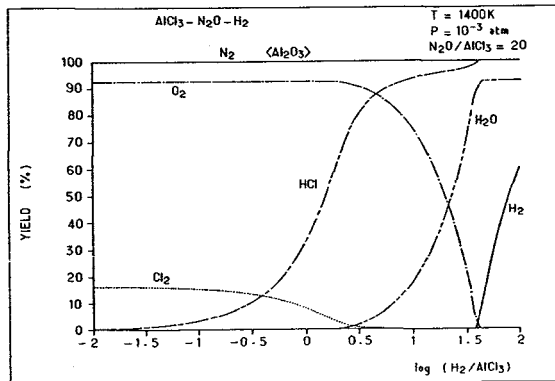


Figure 3 :
Variation of η_x equilibrium yields for the main species as a function of κ , with $\alpha=20$, $P=10^{-3}$ atm (101 Pa) and $T=1400K$.

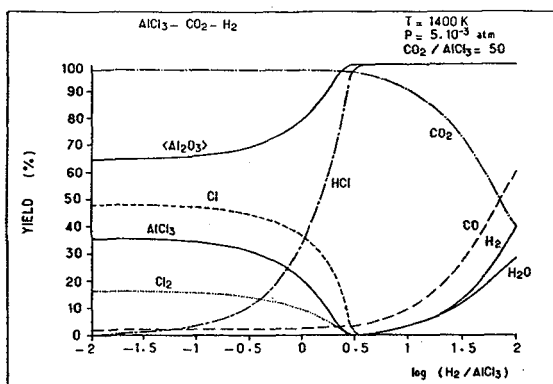


Figure 4 :
Variation of η_X equilibrium yields for the main species as a function of κ , with $\beta=50$, $P=5 \cdot 10^{-3} \text{ atm}$ (506 Pa) and $T=1400 \text{ K}$.

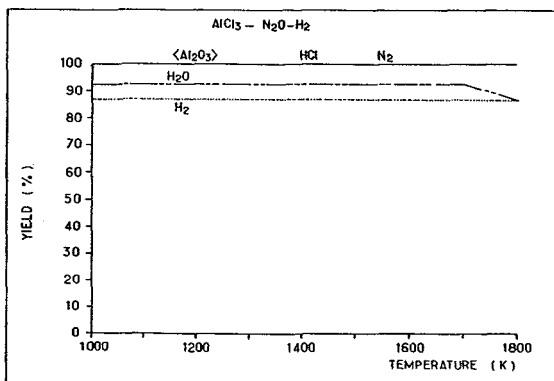


Figure 5 :
Variation of η_X equilibrium yields for the main species as a function of temperature with $\alpha=20$, $\kappa=150$, $P=10^{-3} \text{ atm}$ (101 Pa) and $T=1400 \text{ K}$.

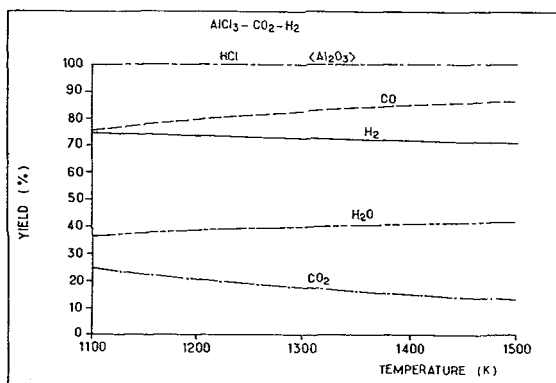


Figure 6 :
Variation of η_X equilibrium yields for the main species as a function of temperature with $\beta=50$, $\kappa=150$, $P=5 \cdot 10^{-3} \text{ atm}$ (506 Pa) and $T=1400 \text{ K}$.

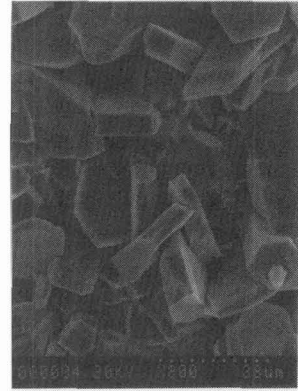
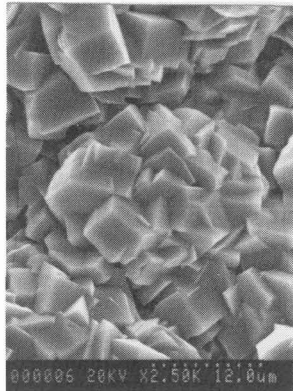
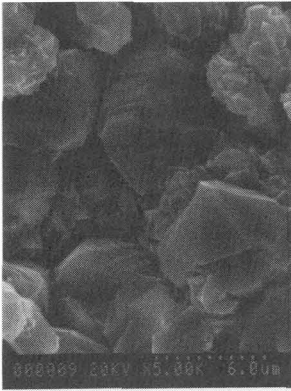


Fig.7. Fig.8. Fig.9.
SEM micrographs showing the microstructure of
Fig.7. $\alpha\text{-Al}_2\text{O}_3$ and $\theta\text{-Al}_2\text{O}_3$ at $T=1000^\circ\text{C}$.
Fig.8. $\alpha\text{-Al}_2\text{O}_3$ at $T=1150^\circ\text{C}$.
Fig.9. $\alpha\text{-Al}_2\text{O}_3$ at $T=1200^\circ\text{C}$.

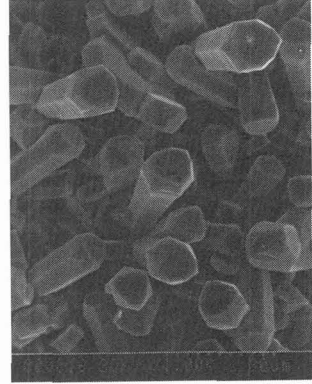
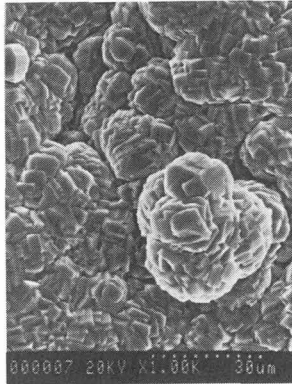
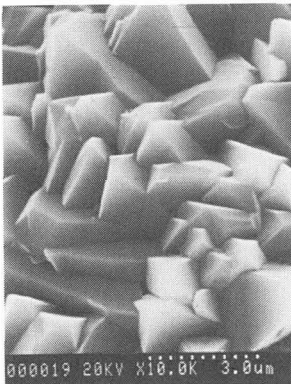


Fig.10. Fig.11. Fig.12.
SEM micrographs showing the microstructure of
Fig.10. $\alpha\text{-Al}_2\text{O}_3$ at $T=1100^\circ\text{C}$.
Fig.11. $\alpha\text{-Al}_2\text{O}_3$ at $T=1200^\circ\text{C}$.
Fig.12. $\alpha\text{-Al}_2\text{O}_3$ at $T=1300^\circ\text{C}$.